MATHEMATICAL BIOSCIENCES
AND ENGINEERING
Volume **2**, Number **3**, August **2005**

http://www.mbejournal.org/

pp. **611–622**

MODELING MULTICELLULAR SYSTEMS USING SUBCELLULAR ELEMENTS

T. J. Newman

Department of Physics & Astronomy, and School of Life Sciences,
Arizona State University, Tempe, AZ 85287

Abstract. We introduce a model for describing the dynamics of large numbers of interacting cells. The fundamental dynamical variables in the model are subcellular elements, which interact with each other through phenomenological intra- and intercellular potentials. Advantages of the model include i) adaptive cell-shape dynamics, ii) flexible accommodation of additional intracellular biology, and iii) the absence of an underlying grid. We present here a detailed description of the model, and use successive mean-field approximations to connect it to more coarse-grained approaches, such as discrete cell-based algorithms and coupled partial differential equations. We also discuss efficient algorithms for encoding the model, and give an example of a simulation of an epithelial sheet. Given the biological flexibility of the model, we propose that it can be used effectively for modeling a range of multicellular processes, such as tumor dynamics and embryogenesis.

1. **Introduction.** Computational modeling of multicellular systems has become an increasingly useful tool for the interpretation and understanding of experimental data in a variety of biological areas. Numerous studies have been performed within the modeling community, with application to collective dynamics of unicellular organisms, such as myxobacteria [13] and slime molds [16, 28], and to dynamics within multicellular organisms. Studies of the latter include avascular tumor growth [3, 26], tumor angiogenesis [4], embryogenesis [5, 20], and cell sorting [7, 10].

A fundamental issue in modeling cell populations is that of scale. One is typically interested in systems composed of tens of thousands to many millions of cells, and yet the cell population is often phenotypically heterogeneous. Therein lies the problem of whether or not to include more biological realism at the cellular level, with the inevitable computational cost of being limited to smaller numbers of cells. The different modeling techniques currently employed can be viewed as different compromises to this inescapable problem. At the most coarse-grained level one erases cell identity and uses continuous cell densities to describe the system. The classic model of this type is the Keller-Segel differential equation model of aggregation in social amoeba [14]. Similar differential equation models have been applied to many other areas, including, of course, tumor growth [3, 4, 18]. Cell densities can also be modeled using finite element methods [5]. At the next finer scale, cells within the population are modeled as discrete objects, yet with little or no internal structure [2, 19]. Such models may be constructed either as cellular

2000 *Mathematics Subject Classification.* 92C10, 92C15, 82C31.

Key words and phrases. tumor growth, development, embryogenesis, epithelial sheet, computer simulation, multicellular systems, Langevin dynamics.

automata on a grid, or else as many-body simulations with no underlying lattice. Recent work has indicated that in the presence of chemotaxis, grid effects can lead to strong artifacts. Proceeding to smaller length-scales, cells are endowed with a size (which can change with time during the cell cycle), and perhaps anisotropy (e.g. modeled as ellipsoids) to mimic cell shape and/or cell polarity [7, 21]. An ingenious and popular model of this type is that due to Graner and Glazier, in which cells are represented as clusters of Potts spins on a fine grid [10]. The Potts model approach has been applied to a wide range of systems, including cell sorting [8], slug formation in *Dictyostelium* [16], and avascular tumor growth [26]. At smaller scales still, the internal biochemical or biomechanical dynamics of the cell are included, e.g. signal transduction for response to chemical signals, and/or cytoskeleton dynamics via actin polymerization [9, 23]. As the scale of biological detail becomes finer, computational constraints limit the size of the cell population. Indeed, models primarily concerned with cytoskeleton dynamics typically focus on a single cell.

In this paper we introduce a framework for modeling multicellular systems which is designed to allow simulation of large numbers of cells in three dimensions, but which also allows for adaptive cell-shape dynamics and the accommodation of successive degrees of intracellular biology. This framework uses "subcellular elements" (defined below) as the fundamental dynamical variables, along with overdamped Langevin dynamics [19, 27] for temporal development of the system.

The outline of the paper is as follows. We describe the subcellular element model in the next section. In section 3 we use a succession of mean-field approximations to connect our model to more coarse-grained descriptions. In section 4 we briefly discuss efficient implementation of the model and give a simple example of numerical output. We conclude in section 5 with a summary of the main results of the paper and a discussion of biological extensions of the model.

2. **The subcellular element model.**

The cell sets the fundamental scale in multicellular systems. As such, it is natural to base model descriptions of these systems at the cellular scale. One of the key properties to incorporate in a cell-based model is dynamical change in cell shape (or, more generally, cell polarity), which can occur in response to local mechanical interactions with neighboring cells, or in response to long-ranged chemical signaling [1]. Adaptive changes in cell shape and cell polarity allow coherent dynamics of large numbers of cells. For example, several mechanisms of large-scale morphological change during gastrulation are due to cell intercalation, which is driven by elongation of individual cells along a particular axis [29]. From a modeling perspective, cell shape is difficult to parameterize. For instance, systematically extending an ellipsoid model of cells in three dimensions requires complicated geometrical constructions. Ideally, one would like a model in which cell shape emerges from cellular interactions – in other words, for cell shape to be adaptive to the local environment. Here, we attempt to instantiate this property by sub-dividing each cell into a number of subcellular elements. Both the intra- and intercellular dynamics are written in terms of interactions between these elements. We shall first describe this dynamics by writing the equations of motion for the elements, and then discuss how this dynamics can be interfaced with the underlying biology.

For simplicity, consider a system with a constant number N of cells in three spatial dimensions, with each cell being composed of M elements. We label an

individual cell by $i \in (1, N)$ and an element in cell i by $\alpha_i \in (1, M)$. For ease of discussion we assume that chemical signaling is absent from the system, so that cells respond purely to local biomechanical interactions. In this case, the position vector of element α_i is taken to change in time according to three processes: (i) a weak stochastic component, which mimics the underlying fluctuations in the dynamics of the cellular cytoskeleton; (ii) an elastic response to intracellular biomechanical forces; and (iii) an elastic response to intercellular biomechanical forces. We assume further that the elements' motion is over-damped, so that inertial effects can be ignored. The equation of motion for the position vector of element α_i takes the form:

$$\dot{\mathbf{y}}_{\alpha_i} = \eta_{\alpha_i} - \nabla_{\alpha_i} \sum_{\beta_i \neq \alpha_i} V_{\text{intra}}(|\mathbf{y}_{\alpha_i} - \mathbf{y}_{\beta_i}|) - \nabla_{\alpha_i} \sum_{j \neq i} \sum_{\beta_j} V_{\text{inter}}(|\mathbf{y}_{\alpha_i} - \mathbf{y}_{\beta_j}|) \ . \quad (1)$$

On the right-hand side, the noise term η_{α_i} is a Gaussian-distributed random variate with zero mean and correlator

$$\langle \eta^m_{\alpha_i}(t) \eta^n_{\beta_j}(t') \rangle = 2\nu \delta_{i,j} \delta_{\alpha_i, \beta_j} \delta^{mn} \delta(t - t') \ , \quad (2)$$

where m and n are vector component labels in the three-dimensional space. The second and third terms on the right-hand side of equation (1) represent, respectively, intra- and intercellular interactions between the elements. These interactions are completely characterized by the phenomenological potentials V_{intra} and V_{inter}. At this level of description, all relevant biological detail must be encoded into these two potentials. The elemental composition of cells, along with the inter-elemental potentials, are shown schematically in Figure 1. We have assumed that "two-body" potentials are sufficient to describe the dynamics. It may be necessary to use "three-body" potentials to capture the essence of more complicated interactions.

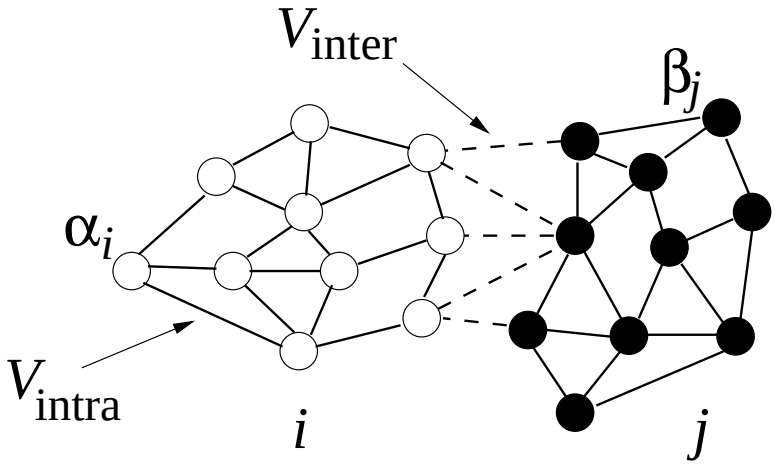

FIGURE 1. Schematic diagram showing two cells, i and j, and a subset of the intra- and intercellular interactions between their elements. The elements of cell i are represented by open circles, and those of cell j by filled circles. The intra- and intercellular interactions are represented by solid and dashed lines respectively.

For given biological applications of this modeling framework, one must intuit (or, better, derive) reasonable forms for V_{intra} and V_{inter}. For illustrative purposes,

consider a population of cells which are weakly adhesive to one another. Subcellular elements both within and between cells will be mutually repulsive if their separation is below the equilibrium size of an element. For separations larger than this size, the elements will be mutually attractive, but with the strength of attraction falling off rapidly with separation. These properties can, for example, be conveniently encoded via a generalized form of the Morse potential, which is commonly used in physics and chemistry to model inter-molecular interactions [24]. The (generalized) Morse potential has the explicit form

$$V(r) = U_0 \exp(-r/\xi_1) - V_0 \exp(-r/\xi_2) \ , \tag{3}$$

and is illustrated in Figure 2. It is straightforward to evaluate the position and depth of the attractive potential minimum in terms of the four parameters (U_0, V_0, ξ_1, ξ_2). In a simple application of the element model, one can use Morse potentials for both V_{intra} and V_{inter}, with parameters chosen to ensure that the former has stronger inter-elemental adhesion than the latter. This condition is necessary, in this simplest version of the model, to maintain the mechanical integrity of the cells.

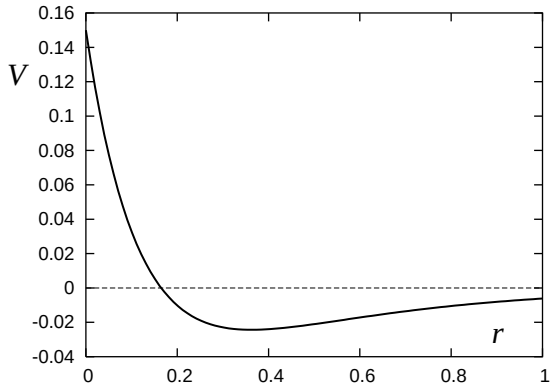

FIGURE 2. The Morse potential for parameter values $U_0 = 0.25$, $V_0 = 0.1$, $\xi_1 = 0.12$, and $\xi_2 = 0.36$, as used for the intracellular potential in section 4.

The introduction and explicit choice of these potentials has so far been purely phenomenological, and some discussion of the biological motivation for these potentials is necessary. Considering a "typical" tissue cell, such as a fibroblast or epithelial cell, the mechanical integrity of the cell is maintained by the internal cytoskeleton [1]. This is a complex network of different types of interconnected filaments, with actin being the most important filament type for cell motility. Dividing the cell into elements corresponds to modeling the shape and mechanical integrity of the cell in terms of volume elements of cytoskeleton. The intracellular attraction between elements arises from the mechanical rigidity of the cytoskeleton, more specifically, the elastic forces transmitted through filaments connecting neighboring elements. These interactions are local, and thus it is necessary that the potential has a rapid decay with distance. Elements at opposite sides of a cell *mechanically* interact through elastic forces mediated by elements comprising the interior of the cell. The biochemical and biomechanical interactions between cells is complex, and arises from a variety of cell-cell (and cell-matrix) contacts, such as

gap, tight, and anchoring junctions [1]. Still, the interactions are local, and, once the cells are linked, one can think of the interaction in terms of a short-ranged elastic potential. There is no reason to favor the Morse potential at this level of description – there are many reasonable potentials that one can write down. Such potentials will, however, be characterized by at least four parameters – two energy scales (for short-ranged repulsion, and intermediate-range adhesion) and two length scales, which characterize the size of an element, and its adhesive range. There are a number of models which have been focused on the detailed mechanics of the cytoskeleton, and its role in cell motility [6, 9, 17, 23]. An interesting subject of future study is the derivation of inter-elemental potentials from coarse-graining the underlying cytoskeletal mechanics considered in these more detailed studies.

3. **Connections to coarse-grained models.** In this technical section we sketch the derivation of coarser-grained models by applying a succession of mean-field approximations to the element model. The essence of this section is summarized in Figure 3, which shows the fundamental objects and fields characterizing the cell models at different scales.

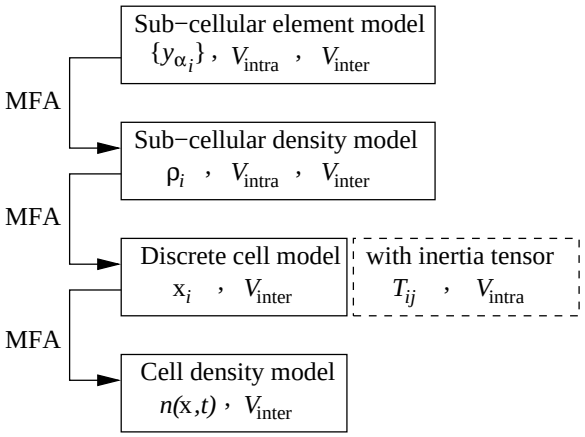

FIGURE 3. Relationships between model descriptions of multicellular systems at different scales. The four levels (from finer to coarser scales) are described explicitly by equations (1), (5), (9), and (10) respectively.

In the first of these coarse-graining steps, we replace the element model by a subcellular density model, in which the discrete elements within a given cell i are replaced by a smooth average density field $\rho_i(\mathbf{x}, t)$. We stress that a separate density field exists for each cell in the system, and that these density fields are strongly correlated to one another. To proceed, we first recast the subcellular element model in terms of the probability distribution of individual elements. We define the probability distribution of element α_i by $P_{\alpha_i}(\mathbf{x}, t) = \langle \delta^3(\mathbf{x} - \mathbf{y}_{\alpha_i}) \rangle$, where the angled brackets denote an average over the noise η. Starting from equations (1) and (2) we use standard methods [19, 27] to derive an equation of motion for

P_{α_i}, which takes the form

$$\begin{aligned}\partial_t P_{\alpha_i}(\mathbf{x},t) = \quad & \nu\nabla^2 P_{\alpha_i}(\mathbf{x},t) \\ + \quad & \nabla\cdot\int d^3x' \ [\nabla V_{\text{intra}}(|\mathbf{x}-\mathbf{x}'|)] \sum_{\beta_i\neq\alpha_i} P_{\alpha_i,\beta_i}(\mathbf{x},t;\mathbf{x}',t) \\ + \quad & \nabla\cdot\int d^3x' \ [\nabla V_{\text{inter}}(|\mathbf{x}-\mathbf{x}'|)] \sum_{j\neq i}\sum_{\beta_j} P_{\alpha_i,\beta_j}(\mathbf{x},t;\mathbf{x}',t) \ , \quad (4)\end{aligned}$$

where P_{α_i,β_j} is the "two-element" distribution function. The equation of motion for this two-element distribution will involve the three-element distribution, and so on. The simplest truncation scheme to break the hierarchy of equations is the mean-field approximation (MFA), in which the statistical correlations between elements are discarded. Within this MFA we have $P_{\alpha_i,\beta_j}(\mathbf{x},t;\mathbf{x}',t) = P_{\alpha_i}(\mathbf{x},t)P_{\beta_j}(\mathbf{x}',t)$.

We now define the subcellular density of cell i via $\rho_i(\mathbf{x},t) = \sum_{\alpha_i} P_{\alpha_i}(\mathbf{x},t)$. Summing over α_i in equation (4), and imposing the MFA, we find a closed equation for this subcellular density function, which takes the form of an advection-diffusion equation:

$$\partial_t\rho_i(\mathbf{x},t) = \nu\nabla^2\rho_i(\mathbf{x},t) + \nabla\cdot\rho_i(\mathbf{x},t)\nabla\Phi_i(\mathbf{x},t) \ , \quad (5)$$

where the velocity potential experienced by the density field of cell i is given by

$$\Phi_i(\mathbf{x},t) = \int d^3x' \ V_{\text{intra}}(|\mathbf{x}-\mathbf{x}'|)\rho_i(\mathbf{x}',t) + \int d^3x' \ V_{\text{inter}}(|\mathbf{x}-\mathbf{x}'|)\sum_{j\neq i}\rho_j(\mathbf{x}',t) \ . \quad (6)$$

The MFA used to derive this density equation will typically be good when the number of elements used to define the cell is very large. The density representation may well be interesting to explore from an analytical standpoint; however, it is probably not so useful for numerical implementation. For simulation of N cells, one must simultaneously integrate N coupled partial differential equations on a fine three-dimensional grid. As we shall see in the next section, the underlying element model, expressed in equation (1), can be very efficiently encoded for simulation with no need of an underlying grid.

We take this opportunity to mention that equation (5) can be discretized in such a way that it resembles a master equation [11]. In this representation, the density of cell i can be interpreted as a probability distribution of identical elements, which move from one grid site to the next by activated hopping. The hopping rate has the Arrhenius form $\sim \exp(-\Delta\Phi_i/2\nu)$ (where $\Delta\Phi_i$ is the change in velocity potential, for an element from cell i, between the two grid sites of interest, which is actually nontrivial to compute since it depends self-consistently on the density ρ_i). The multicellular system as a whole is then defined on a grid, with each grid site able to accommodate (one or more) elements from the N different cells. The elements move about the lattice (and consequently interact) via activated hopping, with highly nonlinear hopping rates as indicated above. This representation, although not easily implemented, illustrates a qualitative connection between a discretized form of the subcellular element model (after one level of MFA) and the lattice-based Potts model [10]. This discretized form of the element model has the flavor of a lattice-gas analog to the Potts model, in the sense that a lattice-based element moves over the lattice and yet keeps its original parent cell identity, whereas a Potts spin is defined at a lattice site and identifies, at a given time, the cell spanning that particular site. Having to hand these two distinct models of multicellular systems (the subcellular element model, as expressed in equation (1), and the Potts model)

defined at similar scales of biological realism, will allow useful cross-validation of these approaches, especially when applied to complicated biological systems.

We can use the density equation (5) to coarse-grain to another scale – where now only gross properties (which we refer to loosely as "moments") of the subcellular density field are used to characterize the cell. This coarse-graining step is analogous to a multipole expansion in electromagnetism. The zeroth moment of cell i is its mass, which is defined by $m_i(t) = \int d^3x\ \rho_i(\mathbf{x}, t)$. Within the present discussion, this quantity is independent of time and cell index i since we have assumed that all cells have the same number of elements, and that the number of elements does not change with time. Proceeding to the first moment, we define the position vector of the center of mass of cell i via $\mathbf{x}_i(t) = \int d^3x\ \mathbf{x}\rho_i(\mathbf{x}, t)$. The equation of motion for this position vector is obtained from equation (5) and takes the form

$$\dot{\mathbf{x}}_i = -\int d^3x\ \rho_i(\mathbf{x}, t)\nabla\Phi_i(\mathbf{x}, t)\ . \tag{7}$$

We briefly mention the second moment of cell i, namely its inertia tensor [15]. This is defined as $T_i^{mn}(t) = \int d^3x\ \left(x^2\delta^{mn} - x^m x^n\right)\rho_i(\mathbf{x}, t)$. An equation of motion, similar to equation (7), can be written down for this tensor. This quantity contains crucial information regarding the *mechanical polarity* of the cell. Higher-order moments can be defined and contain successively more information about the shape and density distribution of the cell.

Since the equations of motion of these moments are written in terms of integrals over the subcellular density, they are all strongly inter-dependent. To write closed equations again requires some form of truncation. Here we use the simplest, which is again a form of MFA; namely, $\int d^3x\ f(\mathbf{x})\rho_i(\mathbf{x}, t) = f(\mathbf{x}_i(t))$. This allows us to express the right-hand side of equation (7) in terms of $\mathbf{x}_i(t)$, and we find the closed equation

$$\dot{\mathbf{x}}_i(t) = -\nabla\sum_{i\neq j} V_{\text{inter}}(|\mathbf{x}_i(t) - \mathbf{x}_j(t)|)\ . \tag{8}$$

There are two interesting points to note: (i) the intracellular potential has vanished under this approximation, since we are essentially shrinking the cells to points, and (ii) the dynamics are now deterministic. Concerning the first point, the intracellular potential will reappear in this coarse-grained description if we include second-order effects – namely, if we derive two coupled equations for each cell, describing the time-dependence of the cell's position vector and its inertia tensor. Concerning the second point, the effect of the noise η_{α_i} has vanished since the first MFA leading to equation (5) essentially assumes an infinite number of elements, so that the explicit noise terms are averaged to zero. The noise from a finite number (M) of elements will be nonzero, and have a variance which scales as $1/M$. This weak noise (which describes the random wandering of the center of mass) can be added to equation (8) *a posteriori* in order to retain stochasticity in this discrete cell representation. One can then write equation (8) as

$$\dot{\mathbf{x}}_i(t) = \eta_i(t) - \nabla\sum_{i\neq j} V_{\text{inter}}(|\mathbf{x}_i(t) - \mathbf{x}_j(t)|)\ , \tag{9}$$

where the noise η_i has zero mean, and correlator $\langle\eta_i^m(t)\eta_j^n(t')\rangle = 2D\delta_{i,j}\delta^{mn}\delta(t-t')$, where $D = \nu/M$. This stochastic model, which tracks the positions of the cells, is precisely that studied by Newman and Grima [19]. As shown in that work, a further MFA applied to equation (9) leads to a closed equation for the density of

cells, which is defined as $n(\mathbf{x},t) = \sum_i \langle \delta^3(\mathbf{x} - \mathbf{x}_i(t))\rangle$. We omit the details here and simply give the final result:

$$\partial_t n(\mathbf{x},t) = D\nabla^2 n(\mathbf{x},t) + \nabla \cdot n(\mathbf{x},t)\nabla\Psi(\mathbf{x},t) \ , \tag{10}$$

where the coarse-grained velocity potential Ψ for the cell density has the form

$$\Psi(\mathbf{x},t) = \int d^3x' \ V_{\text{inter}}(|\mathbf{x} - \mathbf{x}'|)n(\mathbf{x}',t) \ . \tag{11}$$

A rigorous derivation of this last step has been given by Stevens in the context of chemotaxis [25], and uses the limit of infinite cell number, with an appropriately scaled chemotactic coupling.

Finally, after three levels of coarse-graining, we have arrived at a partial differential equation for the cell density, as given in equations (10) and (11). As mentioned in the introduction, this level of description has been widely used to describe the large-scale dynamics of cell populations. However, as should be clear from this analysis, a great deal of statistical information and smaller-scale biomechanics must be discarded at this scale. It would be very interesting to rederive the density equations from a more careful analysis. Some details of the intracellular potentials (especially regarding cell polarity) can be captured in this largest-scale description through i) calculating renormalized parameters, such as the diffusion coefficient D, in the density description (10), and ii) deriving the companion equation for a "cell-polarity field" from the discrete cell equations for the inertia tensor.

4. **Efficient algorithms and model output.** We now return to the subcellular element model as described in section 2. The numerical implementation of this model turns out to be fairly straightforward and efficient. Since the fundamental dynamical variables are position vectors, we have no need for an underlying grid, and simply need to track the values of the $(M \times N)$ vectors $\{\mathbf{y}_{\alpha_i}\}$ which completely describe the state of the system at any given time.

It is worth mentioning that some care must be taken in constructing the algorithm so as to avoid a CPU cost which scales as $(MN)^2$. This would arise from attempting to interact every element with every other in order to update the system. Clearly this is not necessary since the potentials are short-ranged. As such, the algorithm only needs to interact a given element α_i with those elements which are close enough to have a nonnegligible interaction. As long as we can efficiently identify these nearby elements, our algorithm will have a CPU cost which scales as MN. This will allow the simulation of large numbers of cells with moderate to large numbers of elements per cell. There are a number of ways to identify nearby elements. The methods to achieve this have been developed over the years in molecular dynamics simulations [12, 22]. Examples are neighbor tables and the more sophisticated binary search trees and octrees. We have employed a method based on "sectors." The three dimensional system is broken up into a grid of sectors – the size of a sector chosen to be about twice the range of inter-elemental interactions. The dynamics of the elements are completely oblivious to the sectors. The sectors simply allow one to construct a look-up table, wherein for each sector there is a list of the identity of those elements in that sector. When one calculates the interactions of a given element, one computes the interactions between that element and all those in its own sector and the nearest-neighbor sectors. Temporal development is performed using an explicit Euler discretization, with time increment δt.

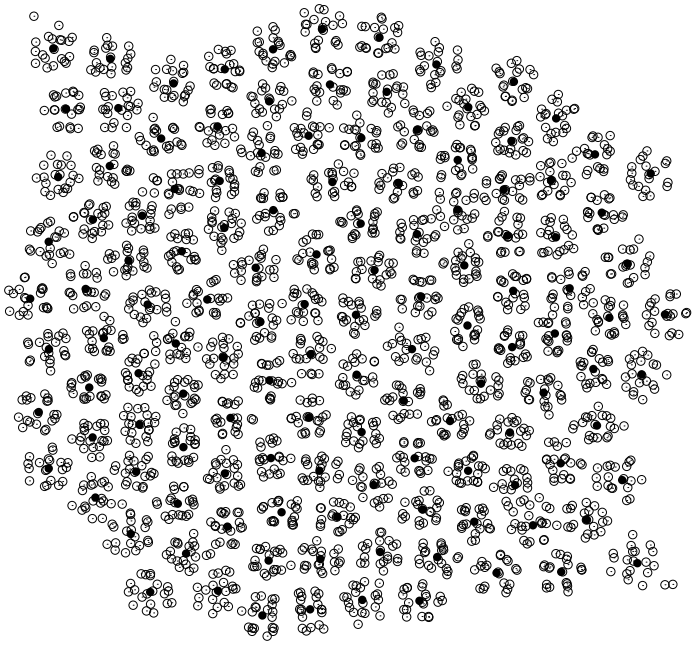

FIGURE 4. An example of numerical output from the model using Morse potentials. Parameter values are given in the main text. Shown here is a two-dimensional *projection* of data from a model of an epithelial sheet. Each of the 128 cells is composed of 20 elements (open circles), and element motion is constrained in the third dimension by hard-wall boundaries. The filled circles indicate the center of mass of each cell.

In Figure 4 we show an example of the output of this algorithm. In this example we have simulated 128 cells, with each cell constructed from 20 subcellular elements. Both the intra- and intercellular potentials are chosen to be generalized Morse potentials, with parameter sets $(U_0, V_0, \xi_1, \xi_2) = (0.25, 0.1, 0.12, 0.36)$ and $(0.25, 0.05, 0.12, 0.24)$, respectively. Other parameter values are $\nu = 0.001$ and $\delta t = 0.1$. For ease of presentation we have simulated the cells in a quasi-two-dimensional geometry, with hard-wall boundary conditions at $z = 0$ and $z = 0.5$, which might represent an epithelial layer bounded by a basement membrane. The system is shown after about 3,000 iterations, starting from a random distribution of cell positions (with the initial positions of the elements for each cell randomly distributed in a small region about these cell positions). This simulation requires about three minutes on a 2GHz PC. Extrapolating to larger systems, we see that thousands of iterations for a system of $10,000$ cells (each with 20 elements) requires a few hours of CPU time on a PC. More sophisticated optimization of the algorithm will allow further improvements in efficiency. Note that as a result of the elements attempting to form intercellular adhesive bonds with elements of nearby cells, the cells have adapted their cell shapes to their local biomechanical environment. A more systematic numerical study comparing the different coarse-grained descriptions is currently in progress.

5. **Summary and outlook.** In this paper we have introduced a model of interacting multicellular systems, in which the fundamental objects are not cells, but subcellular elements – by which we mean, in the simplest sense, small volume elements of intracellular cytoskeleton. The dynamics of the elements is described by Langevin equations, as given in equation (1). The three dynamical contributions to a given element's motion are (i) a weak stochastic component; (ii) local biomechanical interactions with other elements within the same cell, described by a phenomenological potential V_{intra}; and (iii) local biomechanical interactions with elements in nearby cells, these described by a potential V_{inter} (see Figure 1). The success of the model in a given biological application depends, in large part, on well-chosen forms of these potentials. The generic form of these potentials is reasonably well captured by the generalized Morse potential (Figure 2). We have outlined, in section 3, a series of coarse-graining procedures (summarized in Figure 3), whereby the subcellular element model can be linked to models at larger scales, such as discrete cell models and differential equation models describing the macroscopic cell density. In section 4 we indicated how an efficient algorithm may be constructed to integrate equation (1) forward in time for large numbers of cells or elements, and gave an example from a simulation of a sheet of cells (Figure 4).

We conclude with a discussion of some of the many possible extensions of the model, whereby biological detail can be added without distortion of the underlying element framework.

5.1. **Cell types.** For simplicity, in this introductory paper we have presented the element model for a population of N identical cells. Phenotypic heterogeneity at the cell level can be described by attaching cell labels to the noise strength ($\nu \to \nu_i$), intracellular potentials ($V_{\text{intra}} \to V_i$), and intercellular potentials ($V_{\text{inter}} \to V_{i,j}$).

5.2. **Subcellular element types.** For many applications it will not be sufficient to construct a cell from M identical elements. For instance, it might be necessary to distinguish elements in the interior of the cell ("cytoplasmic elements") from elements on the surface of the cell ("membrane elements"). Different element types can easily be instantiated by defining the appropriate classes of intra- and intercellular potentials. In the example just given, the intercellular interactions would primarily be described by an intercellular potential connecting membrane elements from neighboring cells, while the cytoplasmic elements would interact only with elements within the same cell. In addition, elements can be endowed with internal variables registering environmental variables such as pH or nutrient level, and communicate these variables to neighboring elements to trigger appropriate cell response.

5.3. **Extracellular element types.** Cells not only adhere to each other, but also interact biomechanically with a range of non-cellular environmental structures, such as the extracellular matrix or various gel-like media [1]. In some cases these structures are produced by the cells themselves. Within the spirit of the element model, these extracellular structures can also be constructed from elements (i.e. elastically coupled degrees of freedom on the same length-scale as the subcellular elements) with appropriately defined interaction potentials to describe the cell/non-cell interactions.

5.4. **Chemotaxis.** We have been exclusively concerned with short-ranged biomechanical interactions in this paper. Equally important for many applications (e.g.

embryogenesis, wound healing) are long-ranged chemical interactions. The simplest way to introduce such interactions in the element model is to chemically couple the centers of mass of cells which are signaling to one another. Then, since the source and sink of the signal are points, it is straightforward to implement the Green function methods developed in some detail in Newman and Grima [19]. These methods encode the diffusion of chemical signals through the diffusion equation Green function (which allows one to avoid introducing a fine grid for explicit integration of the chemical diffusion equations). More sophisticated treatments would be based on cell polarity induced by the chemical signal. For instance, one could use chemically responsive element types within the cell, so that the cell as a whole responds to a chemical signal via a subcellular element response, followed by a cell-level response mediated by elastic interactions between responsive and non-responsive elements.

5.5. **Cell cycle.** For many applications, and in particular that of tumor growth, cells in the population are undergoing numerous cell divisions over the time scales of interest. Cell growth can be accommodated in the modeling framework by allowing new elements to be spawned within the cell (based on, for instance, an internal monitoring of nutrient levels as discussed above in subsection 5.2). Mitosis is more complicated, and we here describe a simple mechanism to achieve this, although more realistic dynamics may be necessary in particular applications. To capture the biological essence of mitosis, one can define a spindle axis in the cell, which then defines a plane separating the two future daughter cells. One can then turn off intracellular interactions between elements on either side of this plane to initiate cell division.

In this final section we have tried to give a flavor of possible biological extensions of the model, and the ease with which they can be implemented within the element framework. This flexibility must ideally be tempered by minimal incremental model-building in order to keep models simple enough to understand from both quantitative and biological perspectives. Equally important is the need to calibrate and confront the model with real biological data. A first step will be to estimate parameters in the phenomenological potentials using data from force measurements on cytoskeleton mechanics and cell adhesion. Note, such parameterizations will be fairly specific to particular cell types. With these caveats in mind, we hope that the subcellular element model will prove useful in the computational study of a wide range of multicellular systems.

Acknowledgments. The author would like to thank James Glazier, Ramon Grima, John Nagy, Kevin Schmidt, Erick Smith, and Cornelius Weijer for interesting discussions. The author gratefully acknowledges partial support from the NSF (no. IOB-0540680) and NSF/NIH (no. DMS/NIGMS-0342388).

REFERENCES

[1] B. Alberts, A. Johnson, J. Lewis, M. Raff, K. Roberts, and P. Walter, Molecular biology of the cell, 4th ed., Garland, New York, 2004.

[2] T. Bretschneider, B. Vasiev, and C. J. Weijer, A model for *Dictyostelium* slug movement, J. Theor. Biol. **199** (1999), 125-136.

[3] H. M. Byrne, Modeling avascular tumor growth, in Cancer Modelling and Simulation, ed. L. Preziosi, Chapman and Hall/CRC, Boca Raton, Fl., 2003.

[4] M. A. J. Chaplain, Mathematical modeling of angiogenesis, J. Neurooncol. **50** (2000), 37-51.

[5] L. A. Davidson, M. A. R. Koehl, R. Keller, and G. F. Oster, How do sea urchins invaginate – using biomechanics to distinguish between mechanisms of primary invagination, Development **121** (1995), 2005-2018.
[6] P. A. Dimilla, K. Barbee, and D. A. Lauffenburger, Mathematical model for the effect of adhesive mechanics on cell-migration speed, Biophys. J. **60** (1991), 15-37.
[7] D. Drasdo, R. Kree, and J. S. McCaskill, Monte Carlo approach to tissue-cell populations, Phys. Rev. E **52** (1995), 6635-6657.
[8] J. A. Glazier, and F. Graner, Simulation of the differential adhesion driven rearrangement of biological cells, Phys. Rev. E **47** (1993), 2128-2154.
[9] M. E. Gracheva and H. G. Othmer, A continuum model of motility in amoeboid cells, Bull. Math. Biol. **66** (2004), 167-193.
[10] F. Graner, and J. A. Glazier, Simulation of biological cell-sorting using a two-dimensional extended Potts model, Phys. Rev. Lett. **69** (1993), 2013-2016.
[11] R. Grima, and T. J. Newman, Accurate discretization of advection-diffusion equations, Phys. Rev. E **70** (2004), no. 036703.
[12] J. M. Haile, Molecular dynamics simulation: elementary methods, Wiley Interscience, 1997.
[13] O. A. Igoshin, A. Mogilner, R. D. Welch, D. Kaiser, and G. Oster, Pattern formation and traveling waves in myxobacteria: theory and modeling, Proc. Natl. Acad. Sci. (USA) **98** (2001), 14013-14018.
[14] E. F. Keller, and L. A. Segel, Initiation of slime mold aggregation viewed as an instability, J. Theor. Biol. **26** (1970), 399-415.
[15] L. D. Landau and E. M. Lifshitz, Mechanics, 3rd ed., Butterworth-Heinemann, Oxford, 2000.
[16] A. F. M. Maree, and P. Hogeweg, How amoeboids self-organize into a fruiting body: multicellular coordination in *Dictyostelium discoideum*, Proc. Natl. Acad. Sci. USA **98** (2001), 3879-3883.
[17] A. Mogilner and G. Oster, Cell motility driven by actin polymerization, Biophys. J. **71** (1996), 3030-3045.
[18] J. Nagy, The ecology and evolutionary biology of cancer: a review of mathematical models of necrosis and tumor cell diversity, Math. Biosci. Eng. **2** (2005), 381-418.
[19] T. J. Newman, and R. Grima, Many-body theory of chemotactic cell-cell interactions, Phys. Rev. E **70** (2004) no. 051916.
[20] K. J. Painter, P. K. Maini, and H. G. Othmer, A chemotactic model for the advance and retreat of the primitive streak in avian development, Bull. Math. Biol. **62** (2000), 501-525.
[21] E. Palsson and H. G. Othmer, A model for individual and collective cell movement in *Dictyostelium discoideum*, Proc. Natl. Acad. Sci. (USA) **97** (2000), 10448-10453.
[22] D. C. Rapaport, The art of molecular dynamics simulation, Cambridge University Press, 2004.
[23] B. Rubenstein, K. Jacobson, and A. Mogilner, Multiscale two-dimensional modeling of a motile simple-shaped cell, Multiscale Model. Sim. **3** (2005), 413-439.
[24] L. I. Schiff, Quantum mechanics, 3rd ed., McGraw-Hill, Singapore, 1968.
[25] A. Stevens, The derivation of chemotaxis equations as a limit dynamics of moderately interacting stochastic many-particle systems, SIAM J. Appl. Math. **61** (2000), 183-212.
[26] E. L. Stott, N. F. Britton, J. A. Glazier, and M. Zajac, Stochastic simulation of benign avascular tumor growth using the Potts model, Math. Comp. Model. **30** (1999), 183-198.
[27] N. G. van Kampen, Stochastic processes in physics and chemistry, North-Holland, Amsterdam, 1992.
[28] B. Vasiev and C. J. Weijer, Modeling of *Dictyostelium discoideum* slug migration, J. Theor. Biol. **223** (2003), 347-359.
[29] L. Wolpert, R. Beddington, T. Jessell, P. Lawrence, E. Meyerowitz, and J. Smith, Principles of development, 2nd ed., Oxford University Press, Oxford, 2002.

Received on January 1, 2005. Revised on August 3, 2005.

E-mail address: timothy.newman@asu.edu